

Physical Mechanism of Blue-Shift of UV Luminescence of a Single Pencil-Like ZnO Nanowire

Y. H. Yang, X. Y. Chen, Y. Feng, and G. W. Yang*

State Key Laboratory of Optoelectronic Materials and Technologies, Institute of Optoelectronic and Functional Composite Materials, School of Physics Science & Engineering, Zhongshan University, Guangzhou 510275, China

Received July 30, 2007; Revised Manuscript Received October 8, 2007

ABSTRACT

Cathodoluminescence spectroscopy is used to address the ultraviolet (UV) luminescence of a single pencil-like ZnO nanowire whose diameter gradually reduces from bottom to top in the range of 700–50 nm. It is found that the UV emission energy evidently shifts to the high energy with the ZnO nanowire's diameter decreasing and the blue-shift of 90 meV is observed when the nanowire diameter reduces to 50 from 700 nm. The physical mechanism of the UV blue-shift of the ZnO nanowire is attributed to the Burstein–Moss effect under the high carrier concentration.

One-dimensional (1D) nanostructures such as wires, rods, and tubes have become the focus of intensive research due to their unique applications in mesoscopic physics and fabrication of nanodevices.¹ ZnO is a wide band gap (3.37 eV) compound semiconductor with the exciton binding energy of 60 meV and a promising candidate for developing high efficient ultraviolet (UV) laser device at room temperature. Thus, ZnO nanowires have attracted considerable interest because of great potential applications in micro- and nano-optoelectronics.² Generally, the quantum confinement effect can adjust the band gap of nanomaterials when their sizes are smaller than the exciton Bohr radius.^{3–4} Naturally, the so-called blue-shift of luminescence spectra of nanowires with their diameters decreasing is usually attributed to the quantum confinement effect.^{5–7} However, there is a fundamental issue: the diameters of nanowires are much larger than the exciton Bohr radius in most cases of blue-shift,^{5,8,9} in which the quantum confinement effect can be entirely neglected.^{8–9} Therefore, the physical mechanism of blue-shift of luminescence spectra of nanowires with the size far beyond the quantum confinement regime is still unclear. Very recently, Chen et al.⁸ reported the anomalous blue-shift of the luminescence spectrum of ZnO nanorods with the size beyond the quantum confinement regime, which is attributed to the effect of the large surface state of ZnO nanorods with small size. Actually, this is just the energy emission of the surface state of nanowires and not the blue-shift that displays the shift of the free exciton emission to the high energy. In this letter, we report a series of the measurements of the

cathodoluminescence (CL) spectra of a single pencil-like ZnO nanowire whose diameter gradually reduces from bottom to top in the range of 700–50 nm. Interestingly, we observe a 90 meV blue-shift of the UV emission energy when the ZnO nanowire's diameter reduces to 50 from 700 nm. Considering that the size of the ZnO nanowire in our case is far beyond the quantum confinement regime, we suggest that the physical mechanism of the blue-shift of the UV luminescence of a single pencil-like ZnO nanowire seems to be the Burstein–Moss band filling effect under the excitation of the high-energy electron-beam.

Pencil-like ZnO nanowires are prepared on amorphous carbons using thermal chemical vapor transport and condensation without any metal catalysts.^{10–11} Field emission scanning electron microscopy (FESEM), transmission electron microscopy (TEM), and X-ray diffraction (XRD) are employed to characterize the morphology and structure of the prepared sample. CL measurement of a single ZnO pencil-like nanowire is carried out at room temperature using a Gatan Mono-CL system attached FESEM (spot size is about 10 nm) with the accelerating voltage of 25 kV. Figure 1a shows the FESEM image of pencil-like nanowires. Clearly, the diameter of the prepared nanowires gradually reduces from bottom to top in the range of 700–50 nm. The corresponding XRD pattern (Figure 1b) shows that the prepared nanowires are indexed to typically hexagonal ZnO with lattice constants $a = 3.2535 \text{ \AA}$ and $c = 5.2056 \text{ \AA}$. The TEM bright-field image of the sample and the corresponding selected area electronic diffraction (SAD) are shown in Figure 2, in which three parts of a single ZnO nanowire from

* Corresponding author. E-mail: stsygw@mail.sysu.edu.cn.

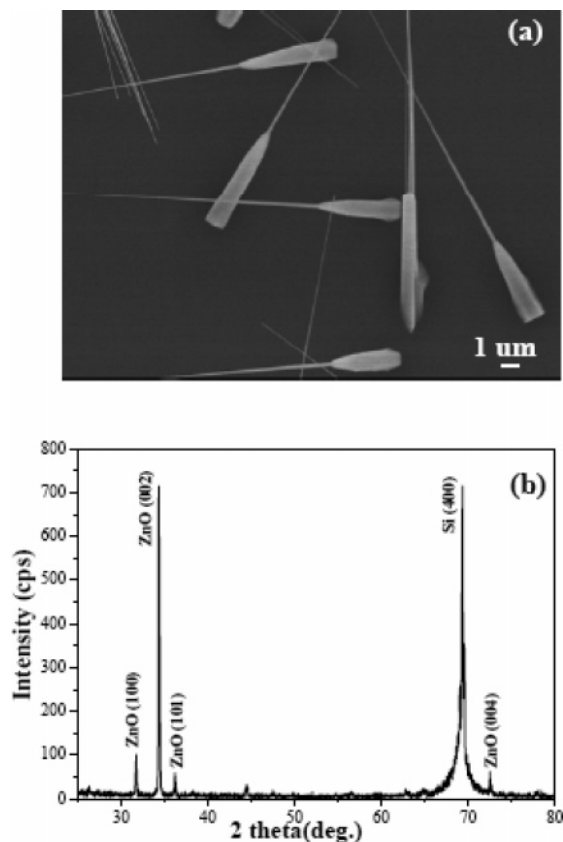


Figure 1. SEM image of pencil-like ZnO nanowires on amorphous carbons (a) and the corresponding XRD pattern (b).

bottom to top are measured. The growth directions of these three parts are the same that is indexed to be [0001], and the space along the growth direction is measured to be 0.52 nm that is coincident with the standard PDF values of (0001) plane of ZnO. These results show that the growth direction of the pencil-like ZnO nanowire is homogeneous and along [0001].

Figure 3a,b shows the FESEM and CL images of a single pencil-like ZnO nanowire. The CL spectrum of six points taken from the different parts of the pencil-like nanowire is shown in Figure 3c. Note that the spot size of the electron-beam is about 10 nm in our CL measurements. Definitely, all six CL spectra exhibit a strong UV emission peak at about 380 nm (3.26 eV) that is attributed to the near band edge (NBE) emission of ZnO. Surprisingly, the UV emission energy shifts to the high energy with the nanowire's size reducing, i.e., there is a clear blue-shift. Figure 3d shows the variation of the UV emission energy and the full width of half-maximum (fwhm) of the UV emission energy as a function of the ZnO nanowire diameter under excited of the electron beam with the accelerating voltage of 25 kV. Meanwhile, an emission peak at 750 nm (1.65 eV) emerges in Figure 3c, which may be caused by the oxygen vacancies of ZnO.

In fact, in the CL case, the irradiation of the high-energy electron-beam could induce the high excitation density in the sample during the CL measurement. Therefore, ZnO nanowires could be excited to the high excitation density under the irradiation of the high-energy electron-beam, which

is enough to produce a lot of carriers during the irradiation. On the other hand, the carrier concentration is an important factor that can greatly influence the band gap energy and then the luminescence spectra.^{12–14} The band gap narrowing (BGN) effect and the Burstein–Moss (BM) effect often appear in the semiconductors with the high carrier concentration.^{15–16} The BGN effect will cause the decrease of the band gap width, because the electron–electron repulsive interaction and the localization of the electron wave function become weak by the screening of the potential due to the presence of many electrons. The BM effect is an important phenomenon in n-type semiconductors which can cause the enlargement of the band gap in the absorption and photoluminescence spectra.¹⁷ As shown in Figure 4a,b, when the carrier concentration in semiconductors is high enough, the Fermi level will move into the conduction band due to the filling of the conduction band by electrons, and then the absorption can only occur between the valance bands and about or above the Fermi level. Note that, the BM shift would not appear when the carrier concentration is below a critical value, and the BGN effect dominates when the carrier concentration is lower than the critical value of the BM effect.¹⁶ When the carrier concentration is high enough, the BM shift is much larger than that of the BGN effect and is dominant in the luminescence spectra, which leads to a blue-shift of UV luminescence. Under the condition of the high carrier concentration, the BM shift (ΔE_{BM}) of the band edge absorption in the n-type semiconductor is given^{16–17}

$$\Delta E_{\text{BM}} = \left(1 + \frac{m_e^*}{m_h^*} \right) \left(\left(\frac{3}{\pi} \right)^{2/3} \frac{h^2}{8m_e^*} n^{2/3} - 4KT \right) \quad (1)$$

where h is the Planck constant, K is the Boltzmann constant, T is the absolute temperature, n is the electron carrier concentration in the conduction band, m_e^* and m_h^* are the effective masses of electron and hole, respectively. Here, we set $m_e^* = 0.28m_0$ and $m_h^* = 0.59m_0$.¹⁸ Thus, the energy of the band gap increases with the carrier density increasing.

In our experiments, we use the electron-beam with 25 kV to excite six points on a single pencil-like ZnO nanowire whose diameter gradually decreases from bottom to top. Therefore, the excitation density of each point increases with the diameter decreasing. When the carrier concentration created by the high excitation density is high enough, the BM effect will be dominant under the high-energy electron-beam excitation. In other words, the blue-shift will occur as our observation in this case. In detail, the energy injected into the nanowire will cause loss of oxygen and stoichiometric disturbances in the ZnO lattice when ZnO is excited by the high-energy electron-beam. Since ZnO is naturally an n-type semiconductor, the Fermi level will move into the conduction band when there is loss of oxygen.¹⁹

Generally, electrons that are injected into ZnO nanowires will transport and excite the secondary-electrons until their energy exhausts. Meanwhile, some secondary electrons with the higher energy can excite the secondary electrons too. Therefore, the excited density is relatively large. The carrier

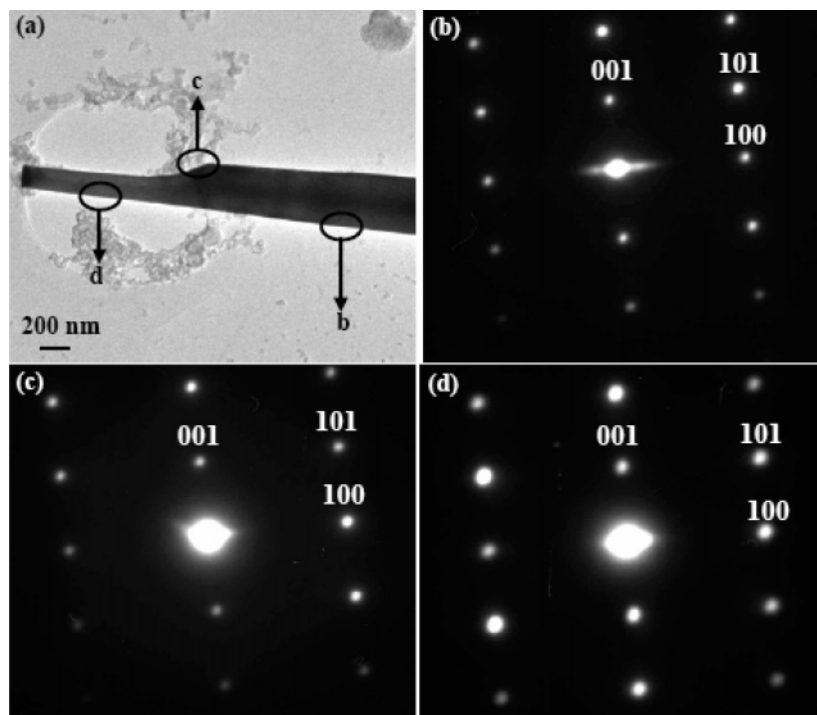


Figure 2. TEM bright-field image (a) and the corresponding SAD patterns (c and d) of a single pencil-like ZnO nanowire.

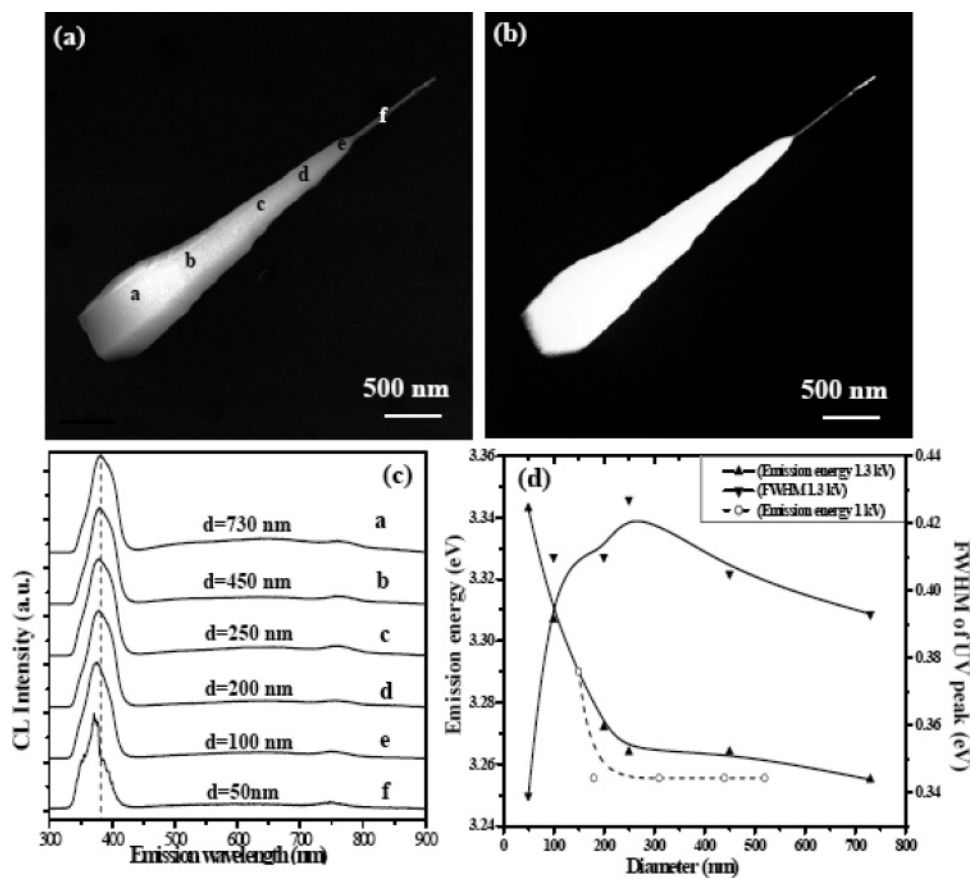


Figure 3. FESEM (a) and CL (b) images of a single pencil-like ZnO nanowire and the corresponding intensity normalized CL emission spectra (c) of six points marked in (a). The variation of the UV emission energy and the full width of half-maximum of the UV emission energy as a function of the ZnO nanowire's diameter (d). Additionally, the variation of the UV emission energy of another ZnO nanowire under 1 kV accelerating voltage is shown in (d).

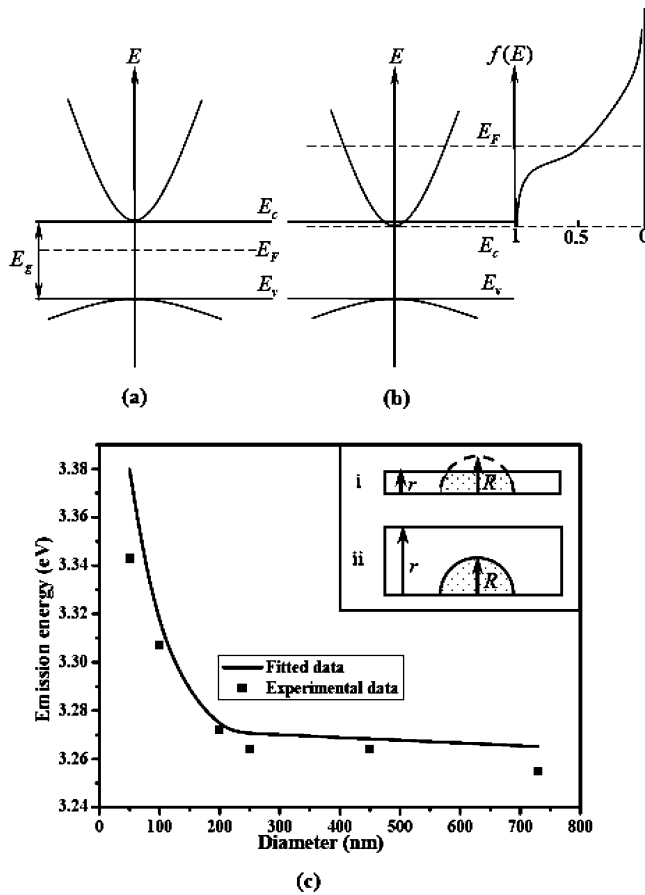


Figure 4. Sketch map of the energy band structure of ZnO (a) and the energy band structure and electron filling when the Burstein–Moss shift happens under the high excited density (b). Comparisons between the experimental data and the theoretical results of the UV emission energy as a function of diameter of ZnO nanowires (c), the inset is the sketch map of the excited volume when the diameter of nanowires is smaller (i) and larger (ii) than R .

concentration of ZnO nanowires can be expressed as follows:

$$n = \frac{N - br}{V} \quad (2)$$

where N is the number of carriers that are excited by the electron-beam, b is the attenuation factor, and r is the diameter of ZnO nanowire. The item of br represents the decrease of the number of carriers during the transport process due to the lattice vibration etc. V represents the excited volume. We assume that the critical depth of excitation is R . When the diameter r is smaller than R , the secondary electrons excited by injected electrons can move to the surface of the material, which makes a continuous excitation by injected electrons possible. Otherwise, the accumulated secondary electrons will prevent incoming electrons from injecting in the material for excitation. V can be described as follows for different situation shown in the inset of Figure 4c

$$\begin{cases} V = \frac{2}{3} \pi R^3, & r \geq R \\ V = \pi r \left(R^2 - \frac{1}{3} r^2 \right) & r < R \end{cases} \quad (3)$$

Substituting eqs 2 and 3 to eq 1, the BM shift (ΔE_{BM}) of the band edge absorption in the n-type semiconductors is attained

$$\Delta E_{\text{BM}} = \left(1 + \frac{m_e^*}{m_h^*} \left(\left(\frac{3}{\pi} \right)^{2/3} \frac{h^2}{8m_e^*} \left(\frac{3(N - br)}{2\pi R^3} \right)^{2/3} - 4KT \right) \right) \quad r \geq R \quad (4)$$

$$\Delta E_{\text{BM}} = \left(1 + \frac{m_e^*}{m_h^*} \left(\left(\frac{3}{\pi} \right)^{2/3} \frac{h^2}{8m_e^*} \left(\frac{N - br}{\pi r \left(R^2 - \frac{1}{3} r^2 \right)} \right)^{2/3} - 4KT \right) \right) \quad r < R \quad (5)$$

Accordingly, eqs 4 and 5 show that ΔE_{BM} will increase with the decrease of the diameter r of ZnO nanowires. According to the experimental results, R of the as-synthesized ZnO nanowire is about 200 nm. Thus, a calculated threshold carrier concentration is fitted to be $4 \times 10^{19}/\text{cm}^3$. Figure 4c shows the fitting result of experimental data based on eqs 4 and 5. Clearly, we can see that the theoretical predictions of our model are well consistent with the experimental data, which means that the proposed model reveals the physical mechanism of the blue-shift of UV luminescence of ZnO nanowires in our case.

Further, the fwhm of UV emission peaks of six points increase with the diameter decreasing, as shown in Figure 3d. When the diameter of ZnO nanowires reaches a critical value, fwhm starts to decrease with the diameter decreasing. This result exhibits the competition between BGN- and BM-induced luminescence, and the BM effect starts to operate and be gradually dominant in the luminescence of the ZnO nanowire along with the diameter decreasing. In addition, the increase of oxygen vacancies will enhance the visible light emission in ZnO. In our case, from Figure 3c, we can see that the intensity ratio of visible and UV light increases with the size of nanowire decreasing, which reflects the increase of oxygen vacancies. Thus, these results further support our model from the change of fwhm.

Additionally, the accelerating voltage of the electron-beam would influence the number of carriers N . Beside the feature of materials, the energy of the injected electron-beam would influence the critical depth R . Therefore, a lower accelerating voltage of the electron-beam will result in the smaller R . Interestingly, our experiments confirm the deductions above. The CL measurements of another ZnO nanowire under 15 kV accelerating voltage are shown in Figure 3d, and the blue-shift starts to appear when the diameter of the ZnO nanowire is less than 200 nm. Note that, under 25 kV accelerating voltage, the remarkable blue-shift can be observed for the ZnO nanowire with a diameter of 200 nm. However, no blue-shift is observed under 15 kV accelerating voltage for the ZnO nanowire with the diameter of 200 nm or more than 200 nm. Therefore, these results show that the blue-shift will disappear with reducing the intensity of the electron-beam

for the ZnO nanowire with a certain size. Accordingly, the BM shift can be affected by the size of nanowires and the energy of the injected electron-beam.

In summary, the blue-shift of the UV energy emission of a single pencil-like ZnO nanowire has been observed in the CL measurement, and a corresponding theoretical model was proposed to be responsible to the unusual blue-shift of nanowires. Based on the experimental and theoretical analyses, the BM effect is suggested to be the physical mechanism of the UV blue-shift of CL spectra of ZnO nanowires.

Acknowledgment. The National Natural Science Foundation of China (50525206) and the Ministry of Education (106126) supported this work. We thank Z. K. Tang of HKUST for a number of useful discussions.

References

- (1) Xia, Y.; Yang, P.; Sun, Y.; Wu, Y.; Mayers, B.; Gates, B.; Yin, Y.; Kim, F.; Yan, H. *Adv. Mater.* **2003**, *15*, 353.
- (2) Heo, Y. W.; Norton, D. P.; Tien, L. C.; Kwon, Y.; Kang, B. S.; Ren, F.; Pearton, S. J.; LaRoche, J. R. *Mater. Sci. Eng. R* **2004**, *47*, 1.
- (3) Yu, H.; Li, J.; Loomis, R. A.; Gibbons, P. C.; Wang, W. L.; Buhro, W. E. *J. Am. Chem. Soc.* **2003**, *125*, 16168.
- (4) Heitmann, J.; Muller, F.; Yi, L.; Zacharias, M.; Kovalev, D.; Eichhorn, F. *Phys. Rev. B* **2004**, *69*, 195309.
- (5) Kim, H. M.; Kim, D. S.; Kim, D. Y.; Kang, T. W.; Cho, Y. H.; Chung, K. S. *Appl. Phys. Lett.* **2002**, *81*, 2193.
- (6) Berezovska, N. I.; Gubanov, V. O.; Dmitruk, I. M.; Biliy, M. M. *J. Lumin.* **2003**, *102–103*, 434.
- (7) Prasad, V.; D'Souza, C.; Yadav, D.; Shaikh, A. J.; Vigneshwaran, N. *Spectrochim. Acta.* **2006**, *65*, 173.
- (8) Chen, C. W.; Chen, K. H.; Shen, C. H.; Ganguly, A.; Chen, C. L.; Wu, J. J.; Wen, H. I.; Pong, W. F. *Appl. Phys. Lett.* **2006**, *88*, 241905.
- (9) Chang, P. C.; Chien, C. J.; Stichtenoth, D.; Ronning, C.; Lu, L. G. *Appl. Phys. Lett.* **2007**, *90*, 113101.
- (10) Yang, Y. H.; Wang, B.; Wang, C. X.; Li, Z. Y.; Chen, D. H.; Chen, J.; Xu, N. S.; Xu, J. B.; Yang, G. W. *Appl. Phys. Lett.* **2005**, *87*, 183109.
- (11) Yang, Y. H.; Wang, B.; Xu, N. S.; Yang, G. W. *Appl. Phys. Lett.* **2006**, *89*, 043108.
- (12) Zhang, D. H.; Gao, R. W.; Ma, L. Y. *Thin Solid Films* **1997**, *295*, 83.
- (13) Roth, A. P.; Webb, J. B.; Williams, D. F. *Phys. Rev. B* **1982**, *25*, 7836.
- (14) Lee, G. H.; Yamamoto, Y.; Kourogi, M.; Ohtsu, M. *Thin Solid Films* **2001**, *386*, 117.
- (15) Jain, S. C.; McGregor, J. M.; Roulston, D. J. *J. Appl. Phys.* **1990**, *68*, 3747.
- (16) Sakai, K.; Kakeno, T.; Ikari, T.; Shirakata, S.; Sakemi, T.; Awai, K.; Yamamoto, T. *J. Appl. Phys.* **2006**, *99*, 043508.
- (17) Burstein, E. *Phys. Rev.* **1954**, *93*, 632.
- (18) Sernelius, B. E.; Berggren, K. F.; Jin, Z. C.; Hamberg, I.; Granqvist, C. *Phys. Rev. B* **1988**, *37*, 10244.
- (19) Hong, R. J.; Huang, B. J.; He, H. B.; Fan, Z. X.; Shao, J. D. *Appl. Surf. Sci.* **2005**, *242*, 346.

NL071849H